Mechanistic insight into the uptake and fate of persistent organic pollutants in sea ice

Jack Garnett[1], Crispin Halsall[1*], Max Thomas[2], James France[2,3,4],
Jan Kaiser[2], Carola Graf[1], Amber Leeson[1], Peter Wynn[1]

1 Lancaster Environment Centre, Lancaster University, Lancaster, LA1 4YQ, UK
2 Centre for Ocean and Atmospheric Sciences, School of Environmental Sciences, University of East Anglia, Norwich Research Park, Norwich, NR4 7TJ, UK
3 British Antarctic Survey, High Cross, Madingley Road, Cambridge, CB3 0ET
4 Department of Earth Sciences, Royal Holloway, University of London, Egham Hill, Egham TW20 0EX, UK

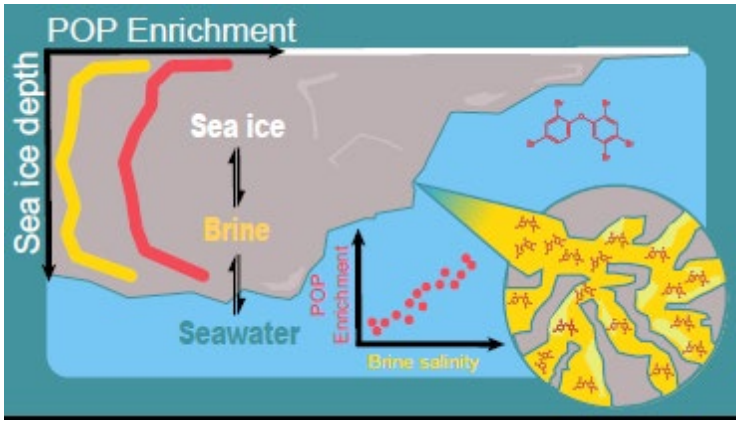

Abstract

The fate of persistent organic pollutants in sea ice is a poorly researched area and yet ice serves as an important habitat for organisms at the base of the marine foodweb. This study presents laboratory-controlled experiments to investigate the mechanisms governing the fate of organic contaminants in sea ice grown from artificial seawater. Sea ice formation was shown to result in the entrainment of chemicals from seawater, and concentration profiles in bulk ice generally showed the highest levels in both the upper (ice-atmosphere interface) and lower (ice-ocean interface) ice layers, suggesting their incorporation and distribution is influenced by brine advection. Results from a 1-D sea ice brine dynamics model supported this, but also indicated that other processes may be needed to accurately model low-polarity compounds in sea ice. This was reinforced by results from a melt experiment, which not only showed chemicals were more enriched in saltier brine, but also revealed that chemicals are released from sea ice at variable rates. We use our results to demonstrate the importance of processes related to the occurrence and movement of brine for controlling chemical fate in sea ice which provides a pathway for exposure to ice-associated biota at the base of the pelagic food web.

1. Introduction

Persistent organic pollutants (POPs) comprise a large group of mainly synthetic, toxic chemicals that have long environmental half-lives and are subject to long-range transport by global atmospheric and oceanic circulation currents [1] . As such, these chemicals are present in the marine environment of polar regions and have been shown to bioaccumulate and biomagnify in Arctic food webs [2, 3] The role of snow and sea ice in the fate and transfer of both older 'legacy' and contemporary 'emerging' chemicals to biological systems has not been well studied despite their occurrence in Arctic seawater. There are now a number of observational studies that have reported relatively high POP concentrations in the remote sea ice snow pack [4-6] and their presence in sea ice itself [7-10].

A warming climate is resulting in substantial changes to the volume and properties of sea ice [11]. There is a strong declining trend in the areal extent of Arctic sea ice cover, which currently ranges between 4 and 16 million km^2 over the annual seasonal cycle [12]. Furthermore, the nature of sea ice is also changing, with the Arctic Ocean now dominated by first-year sea ice (FYI) [13]. As sea ice forms, most of the salts present in the freezing sea water are rejected into the underlying ocean, leaving only small amount entrapped within a network of highly saline brine pockets. As ice continues to grow, more salts are expelled and seasonal meltwater at the surface often 'flushes' the sea ice, reducing its bulk salinity further. Multi-year sea ice (MYI) therefore has a lower bulk salinity and a lower salt flux to the ocean during melt [14] Compared to older MYI, young ice contains more brine per unit volume, and this appears to influence the behaviour and fate of organic micro-pollutants present in the sea ice system [8]. Importantly, many organisms situated at the base of the pelagic food web are abundant in sea ice and inhabit the network of brine inclusions. As the Arctic environment is rapidly changing, there is a rising motivation to understand the biogeochemical cycling of these toxic chemicals in sea ice.

Whilst the presence of POPs such as polychlorinated biphenyls (PCBs) has been established in sea ice [7] most of the recent knowledge on chemical behaviour in sea ice and interactions with seawater and the overlying snowpack has been established through the field observations of Pućko et al., [5, 6, 8, 9, 15, 16] who examined the α- and γ-isomers of hexachlorocyclohexane (HCH) in FYI in the Amundsen Gulf of the Canadian Arctic. The key findings from these studies showed sea ice to have some of the highest concentrations of HCHs measured anywhere in the Arctic. The majority of the HCHs were present in brine, and brine advection influenced the transfer of HCHs between the sea ice, overlying snowpack and underlying seawater.

The aim of this study was to better understand the basic mechanisms governing the uptake and release of organic pollutants in growing and melting sea ice, repectively. We hypothesize

that chemical uptake and distribution is strongly influenced by the formation of brine during sea ice growth and melt. To test this, we performed sea ice growth experiments under controlled laboratory conditions where an artificial 'ocean' was spiked with several persistent organic pollutants. To assess the role of brine in determining their fate, we measured vertical profiles of pollutant concentrations through bulk sea ice samples and made comparisons to predictions from a sea ice brine dynamics model during sea ice formation. We also conducted an experiment to extract brine and assess its composition to examine how organic chemicals are released from sea ice during melt.

2. Materials and methods

2.1. Experimental facility and conditions

The study was conducted in the Roland von Glasow Air-Sea-Ice Chamber (RvG-ASIC) at the University of East Anglia, UK. In essence, the facility consists of a glass-walled tank (approximately 3.5m^3; height: 1.2m; width 1.2m; length 2.5m) located inside an enclosed chamber that can be chilled to –55ºC (see https://www.uea.ac.uk/environmental-sciences/sea-ice-chamber). The tank was filled with artificial sea water (de-ionised water with NaCl – (AksoNobel Sanal-P; purity > 99.5%)). A submerged pump (flow rate: 1000 L h^{-1}) was used to mix the seawater (SW; we refer to it as seawater even though it only contains NaCl). The tank was equipped with an *in-situ* conductivity-temperature sensor (SeaStar DST CTD) along with a series of automated *in-situ* thermistors spanning the depth of the ice profile to measure the ice temperature throughout the experimental periods. Table 1 presents an overview of the experimental conditions for two freeze periods (1 & 2). For the main experiment (Freeze - 1), the air temperature of the chamber was chilled to –35 ºC for 3 days resulting in rapid ice growth and the formation of an ice layer 17±1 cm in depth (uncertainty reflects ice thickness variations across the tank). The ice was subsequently sampled to establish the presence of chemicals in the ice and their distribution throughout the ice column. After the ice had completely melted, 'Freeze - 2' was undertaken with the air temperature set to -18ºC but for a longer duration (7 days) resulting in slower ice growth but with a thicker final ice layer 26±1 cm. The ice sampled during 'Freeze - 2' was also subject to an additional slow-melt experiment to assess chemical behaviour during melt (see Section 2.4.).

Table 1. Experimental conditions and sea ice physical properties for two freeze experiments. Sea ice samples used to assess chemical release in the slow-melt experiment were taken from Freeze - 2 (see section 2.4).

	Freeze - 1	Freeze - 2

Initial NaCl concentration (g L^{-1})	35.4 ± 0.1	35.4 ± 0.1
Air temperature during freezing phase (°C)	-35	-18
Air temperature during melting phase (°C)	5	0
Maximum sea ice depth (cm)	17 ± 1	26 ± 1
Freezing duration (days)	3	7
Coldest recorded temperature in ice (°C)	-13.8	-11.3
Maximum modelled brine salinity (g L^{-1})	178.2*	154.8*
Average ice growth rate (cm d^{-1})	5.7	3.7
Melting phase (days)	6	3

* Derived using the recorded minimum temperature in the sea ice using Equation S1 [17].

An array of chemicals that have been previously observed in the Arctic marine system (see Table 2) and that cover a wide range of physical-chemical properties (Table S1) were spiked into the tank using a stock solution (0.2 to 1.4 μM in 1 L ethanol) to give concentrations between 0.1 and 0.4 nM (Table S2). This was undertaken once the temperature of the seawater had cooled to -1°C to ensure minimal loss of chemicals by volatilisation. The chemical concentrations were up to two orders of magnitude below the estimated aqueous solubilities in seawater (see Table S1), but also up to two orders of magnitude greater than those typically observed in Arctic seawater. The freeze experiments conducted in the facility were performed in darkness to limit the growth of algae and reduce any photochemical loss of the compounds.

2.2. Sampling procedures

Prior to the introduction of chemicals into the chilled seawater, a short period (2 days) of ice growth at –35 ºC permitted samples of seawater (*SW*) (0.2 L; *n* = 3) and bulk ice (*BI*) (3.5 L; *n* = 1) to be collected for the purpose of method blanks. After the ice had melted, the chemical stock spike solution was added and mixed under pumping. A seawater sample (0.2 L, *n* = 1) was taken daily, and triplicate samples (0.2 L; *n* = 3) were obtained on three key days of Freeze - 1 (start: day 1 (before any ice formation); middle: day 4 (once maximum ice had formed);, end: day 11 (after complete ice melt)) to assess analytical precision. Seawater was taken via a pre-installed silicone hose (I.D. 8 mm) with an inlet set at 0.5 m above the base of the tank to avoid interference with any forming ice layer. Bulk ice samples (*n* = 2) were taken once the ice had reached a suitable handling depth using techniques developed by Cottier et al., [18] to limit brine loss and displacement during sampling. Following sampling, ice samples were immediately wrapped in pre-cleaned polyethylene (PE) sheets and transferred to a freezer (–40 ºC) where they were stored prior to further processing. Bulk ice samples were

subsequently sectioned into horizontal layers (0.4 to 1.2 L each; *n* = 9) using a grease-free electric band saw in a cold room (–25 ºC), transferred to individual PE bags and melted at room temperature. Frost Flowers (0.2 L; *n* = 1) present on the surface of the ice were carefully collected using a polyethylene spatula and stored in a freezer before melting for analysis.

2.3. Sample processing and analysis

Salinity was measured in melted sea ice samples, 'slow-melt' aliquots, and melted frost flowers using a calibrated conductivity probe (Hach HQd40 logger with CDC401 probe) after 50 μL of surrogate standard ((^{13}C)PCB-28, (^{13}C)PCB-52, (^{13}C)PCB-180 at 60 pg μL^{-1} in ethanol) was added to each solution. Samples were then subject to solid phase extraction (SPE) using a 12-port vacuum manifold system. Briefly, SPE cartridges (30 mg of 3 cc OASIS HLB) were conditioned using 5 mL of methanol followed by 5 mL of chemical-free purified water (MilliQ; >18 MΩ cm) and then loaded with sample at a rate of 1 to 2 drops per second. Subsequently, the cartridges were centrifuged for 5 minutes at 2000 rpm and later air-dried for a further 40 minutes whilst fitted with an additional cartridge as a precaution against airborne contamination. Cartridges were then soaked with 3 mL of hexane:dichloromethane (1:1) for 5 minutes and eluted with a further 3 mL of this solvent mix. Each sample extract was then subject to a clean-up procedure involving elution through an alumina/silica column followed by gel permeation chromatography (GPC). Samples were then transferred to amber GC vials containing 50 μL of recovery standard (IS) ([^{13}C]PCB-141 [25 pg μL^{-1}] and BDE-69 [75 pg μL^{-1}]) in *n*-dodecane was then added before being reduced under N_2 to a final volume of 50 μL.

Analysis of extracts was performed using a Thermo GC-MS (Trace GC Ultra - DSQ) (Xcalibur software Version 1.4.x) operating in electron impact mode (70 eV) and equipped with an Agilent CP-Sil 8 CB 50 m x 0.25 mm capillary column with 0.12 μm film thickness. A 10-point mixed calibration standard in *n*-dodecane was used for quantification (10 to 450 pg μL^{-1} for OCPs, 10 to 120 pg μL^{-1} for PCBs and 10 to 1250 pg μL^{-1} for PBDEs, respectively). Chemical concentrations presented in this study were corrected for recovery, but not blank corrected. Method detection limits (MDL) were calculated from method blanks (MDL = $\bar{x}_{\text{method blank}} \pm 3 \cdot SD_{\text{method blank}}$) (see Table S3).

2.4. Slow-melt experiment

Following Freeze 2, a separate experiment was conducted (outside of the glass tank but within the coldroom) to examine the release of chemicals from ice during thaw, and to determine how strongly associated each chemical was with brine. Sea ice cores (*n* = 8) were sampled from across the ice slab using a pre-cleaned titanium manual corer (75 mm I.D.). These were

individually split into top (T) and bottom (B) sections of approximately equal length, with each section placed into a separate pre-cleaned PE bag, which were subsequently kept at 0±1 ºC to induce melt, as described by Pućko, et al., [8] and others [19-22]. Sequential meltwater (MW) fractions (0.1 to 1.2 L; *n* = 8) were collected from the respective top and bottom sections and analysed separately (Table S4).

2.5. Calculations and data analysis

Enrichment factors (*EF*) were calculated using Equation 1 to assess the accumulation of chemicals in a particular compartment, relative to seawater. The average chemical concentration of all seawater samples over the experimental period was used for the denominator for each chemical (*SW*; day 1 to day 11). The brine (*BR*) assessed in this study was operationally defined using the average of the first meltwater (*MW*) fraction from both the top and bottom ice sections (MW_{F1T} & MW_{F1B}; *n* = 2) and *FF* is a frost flower sample (taken in Freeze 1). Hence, *EF* values >1 and <1 indicate specific enrichment or depletion, relative to seawater, respectively.

$$EF = \frac{[\text{chemical}]_{\,e.g.\ bulk\ ice\ (BI);\ brine(BR);\ frost\ flower(FF);\ meltwater(MW);}}{[\text{chemical}]_{\,seawater\ (SW)}} \qquad (1)$$

Sea ice depths were normalised to the total sea ice thickness in that experiment (i.e. in Freeze - 1 & 2) to aid comparison between modelled and measured data. A mass-balance calculation was used to assess chemical loss from the system (e.g. volatilisation and/or chamber-side sorption) and evaluate the fraction of chemical present in the various compartments i.e. seawater, bulk ice and brine (at maximum ice depth). Average sea ice concentrations were used to calculate the mass fraction of chemical in the bulk ice, with respect to the total measured mass in the seawater at day 1. The relative standard deviation (RSD) of triplicate seawater samples were used to calculate conservative estimates of the variability of some samples (e.g. frost flowers) (see Table S3). For more information on calculations and data analysis, refer to Equations S1 - S5).

2.6. Brine dynamics model

A 1-dimensional sea ice growth and desalination model was used to predict brine dynamics in a forming sea-ice layer, using the gravity drainage parameterisation presented by [17]. The model is presented in detail in Thomas, et al., [23, 24] where it is has been shown to have predictive capability for the dynamics of brine in sea ice. The brine dynamics parameterization has also been evaluated previously [17]. The model was initialised by prescribing an initial seawater salinity, concentration of a dissolved solute in seawater (e.g. an organic chemical),

sea ice thickness, and ocean mass. For this study, the initial salinity and chemical concentrations were taken from the measured values in the seawater at the beginning of the experiment (i.e. day 1). The model was run with ± 2 s.d. of the initial starting conditions, based on the precision of the measurements of the chemical concentrations in the seawater. The initial sea ice thickness was set to 1cm, and the bulk sea ice salinity and chemical concentrations were set to initial ocean concentrations for all model sea ice layers. The model was forced using measured sea ice temperature profiles, and sea ice thicknesses calculated by extrapolating those profiles back to the measured seawater temperature. In this case, measurements were used instead of a thermodynamic model to minimise errors. Full details including the key equations governing brine salinity (derived using the ice temperature), and how the model simulates brine dynamics (gravity drainage) are presented in the SI.

3. Results and Discussion

3.1. Quality controls & mass-balance

Average recoveries of the surrogate standards were 42 ± 17 % and did not vary significantly between sample type (Table S3). Some blanks contained low levels of several target analytes (e.g. α-HCH γ-HCH, PCB-28, PCB-52) thereby increasing the method detection limits (MDLs) for these compounds. The relative standard deviation (RSD) of triplicate seawater analyses demonstrated precisions of 8 to 40% between all test compounds (see Table S3). Table 2 shows the relative distribution of chemicals in the various compartments of the experimental system on selected days. By day 11, all of the ice had melted and a comparison of the relative mass in the seawater on the initial (day 1) and final (day 11) days of the experiments showed that there was no significant difference ($p > 0.05$; student t-test) for any of the chemicals, indicating negligible losses during the experimental period. Hence, all of the chemicals in the system can be accounted for and are not subject to an artefact of the experimental set-up.

Table 2. Chemical mass (± 1.s.d) apportionment for the experimental compartments on day 1, day 4 and day 11 of Freeze - 1.

Experimental day	Start (day 1)	Middle (day 4)			End (day 11)
Compartment	Seawater	Seawater	Bulk ice	Frost flowers	Seawater
Volume fraction of compartment	100 ± <1	83 ± <1	17 ± <1	<<1%	100 ± <1
NaCl ($\%_{mass}$)	100 ± <1	93 ± <1	7 ± <1	<<1%	100 ± <1
α-HCH ($\%_{mass}$)	100 ± 15	96 ± 18	4 ± 1	<<1%	97 ± 14
γ-HCH ($\%_{mass}$)	100 ± 22	97 ± 34	3 ± 1	<<1%	83 ± 2

PCB-28 ($\%_{mass}$)	100 ± 18	93 ± 10	7 ± 1	<<1%	116 ± 17
PCB-52 ($\%_{mass}$)	100 ± 12	96 ± 14	4 ± 1	<<1%	108 ± 11
Chlorpyrifos ($\%_{mass}$)	100 ± 29	96 ± 32	4 ± 1	<<1%	156 ± 42
BDE-47 ($\%_{mass}$)	100 ± 16	94 ± 64	6 ± 2	<<1%	114 ± 32
BDE-99 ($\%_{mass}$)	100 ± 17	91 ± 48	9 ± 3	<<1%	80 ± 5

Under natural conditions, the transfer of chemicals and salts (e.g. NaCl) can also occur through other pathways such as snow scavenging of airborne pollution and the deposition of sea salt aerosol which serve as an additional source to the sea ice system [4, 5, 15]. However, in this study, airborne sources were negligible (demonstrated by clean blanks). Hence, chemicals present in our experimental sea ice are shown to have originated from the seawater. The results shown in Table 2 from Freeze -1 also show that only a small fraction (3 to 9 %) of the total initial mass of chemicals present in the seawater was entrapped within sea ice during its formation, akin to salt (7%).

3.2. Entrainment of POPs in sea ice.

A time-series for the concentration of NaCl and chemicals in seawater throughout the experiment (day 1 – day 11) can be seen in Figure S1. During the period of sea ice formation (day 1 – day 4) an increase in sea ice thickness and decrease in seawater volume was accompanied by solute rejection from the sea ice, and an increase in the underlying NaCl concentration (from around 35 to 39 g L^{-1}). Given the experimental precision of the measurements made for the organic chemicals seawater (8 to 40 %), it was not possible to establish whether they followed a similar trend to the salt. However, the measured concentrations of salt and all chemicals were markedly lower in bulk ice than seawater, as indicated by the Enrichment Factors ($EF_{BI\text{-}SW} < 1$) presented in Table 3. This finding suggests that organic chemicals are rejected from sea ice throughout ice growth. Interestingly, $EF_{BI\text{-}SW\ [NaCl]} > EF_{BI\text{-}SW\ [POPs]}$ which may indicate preferential rejection of organic chemicals during sea-ice growth.

Despite the low chemical concentrations present in bulk ice, results presented in Table 3 show that $EF_{BR\text{-}SW} > EF_{BI\text{-}SW}$ ($p<0.05$; student t-test), indicating that the chemicals are more strongly associated with the brine fraction and are entrained within the complex network of brine inclusions which extends throughout the ice [25]. Pućko et al., [8] quoted the mean depth-averaged salinity of bulk ice to be 11.6g L^{-1} which gave $EF_{BI\text{-}SW} = 0.4$ for NaCl. Similarly, values for $EF_{BI\text{-}SW}$ were obtained for α-HCH and γ-HCH at 0.4 and 0.5, respectively. The resemblance between this calculated index for NaCl and the two HCH isomers suggests that the levels of

HCH in FYI are probably governed by processes that function to conservatively distribute brine in sea ice. In our study, $EF_{BI\text{-}SW}$ of NaCl resulted in a value of 0.4, although there is a larger range (0.1 – 0.4) between the index for all of the chemicals presented in our study. Natural sea ice is a highly complex medium with marked heterogeneity in physical features over relatively narrow spatial scales (i.e. cms). The chamber ice is markedly younger and thinner than the mid/late-winter Arctic sea ice measured in the field studies above, but the ice formation processes and physical features such as brine channels and frost flowers etc are similar [23]. Some of the differences between our enrichment factors and previous field studies could be due to different temperature and sea-ice growth regimes. However, the higher brine salinity concentrations observed in the Arctic sea ice could have affected organic chemical occurrence and distribution, and is likely to account for differences between the field studies and the chamber ice of this study.

Table 3: Enrichment factors (±1.s.d) for NaCl and chemical contaminants in the different sea ice system compartments. BI=bulk ice; BR=brine; SW=seawater; FF=frost flower; L1= uppermost sea ice layer sampled.

Enrichment Factor	Bulk ice depth(cm)	NaCl	α-HCH	γ-HCH	PCB-28	PCB-52	Chlorpyrifos	BDE-47	BDE-99	Reference
$EF_{BI\text{-}SW}$	17 ± 1	0.4 ± <0.1	0.1 ± <0.1	0.1 ± 0.1	0.2 ± 0.1	0.2 ± <0.1	0.2 ± 0.1	0.1 ± 0.1	0.4 ± 0.2	Freeze -1
$EF_{BI\text{-}SW}$	26 ± 1	0.3 ± <0.1	0.2 ± 0.1	0.3 ± 0.2	0.2 ± 0.1	0.1 ± <0.1	0.3 ± 0.2	0.2 ± 0.1	0.4 ± 0.2	Freeze - 2
$EF_{BI\text{-}SW}$	30	0.4	0.4	0.5	n/m					[8]
$EF_{BI\text{-}SW}$	90	0.2	0.3	0.3	n/m					[9]
$EF_{BI\text{-}SW}$	5	0.3	0.3	0.4	n/m					[9]
$EF_{BR\text{-}SW}$	26 ± 1	1.4 ± <0.1	0.6 ± 0.2	1.0 ± 0.8	1.3 ± 0.5	1.2 ± 0.3	1.2 ± 0.7	0.7 ± 0.5	0.9 ± 0.6	Freeze - 2
$EF_{BR\text{-}SW}$	90	4.4	3.9	4	n/m					[8]
$EF_{FF\text{-}SW}$	n/a	2.3 ± <0.1	0.2 ± 0.1	0.2 ± 0.2	0.2 ± 0.1	0.4 ± 0.1	0.3 ± 0.2	6.6 ± 4.4	24 ± 15	Freeze - 1
$EF_{FF\text{-}SW}$	n/a	< 2.0	0.7	2.1	0.0 – 38.9 $^{\Delta}$					[10]
$EF_{FF\text{-}L1}$	n/a	5.0 ± <0.1	1.5 ± 0.5	2.0 ± 1.5	2.5 ± 0.9	3.0 ± 0.7	2.4 ± 1.4	30 ± 20	50 ± 31	Freeze - 1
$EF_{FF\text{-}L1}$	n/a	< 0.7	1.7 – 68.0 $^{\Delta}$							[10]

n/a=not applicable; n/m=not measured; Δ=different organic chemical used other than that analysed in this study. See Table S5 for values that were used in this literature analysis.

Brine salinity is set by the appropriate *liquidus* relationship [26] and is usually at its respective freezing-point. Changes in the local thermal conditions will cause a corresponding phase-change following this temperature-salinity relationship. Brine salinity measured in Pućko et al.,[8] and in this study was 128 g L^{-1} and 58 g L^{-1}, respectively. Hence, the brine collected in our study was much less concentrated and this is likely to be attributed to differences in sea ice properties (given the age and thickness of the chamber ice) as well as the brine sampling techniques which limited our ability to obtain enough brine for analysis with

a salinity >58 g L^{-1}. These factors most likely contribute to the slightly lower *EF*s measured in this study compared to those calculated from Arctic sea ice [8, 9]. Furthermore, additional pollution sources such as the transfer of chemicals from the overlying snowpack into sea ice and the incorporation of other seawater constituents such as organic matter (dissolved and particulate) may also affect the quantity and distribution of POPs in natural sea ice.

3.3. Distribution of chemicals within sea ice

Figure 1 shows the vertical distribution of salt and chemicals in our chamber-grown sea ice. Data were plotted on a log-scale to show all chemicals and account for their wide range in concentrations. A 'c-shape' profile for bulk salinity (Panel A) is typical for first-year sea ice, whereby elevated concentrations exist at the ice-atmosphere and ice-ocean interfaces. The processes governing the distribution of NaCl in sea ice have been reviewed by Notz and Worster [14]. Due to the crystal structure and the close-packing arrangement of water molecules in ice, there is limited inclusion of solutes (e.g. dissolved ions, particulates etc) within the ice itself [25], but are retained within liquid inclusions between the ice lamellae. Due to surface cooling, brine at the surface of sea ice is colder, more saline, and denser than that below, driving convection currents and facilitating the downward movement of salt-rich brine. This process is better known as gravity drainage and is believed to be the predominant mechanism controlling the removal of salts from the bulk sea ice [14].

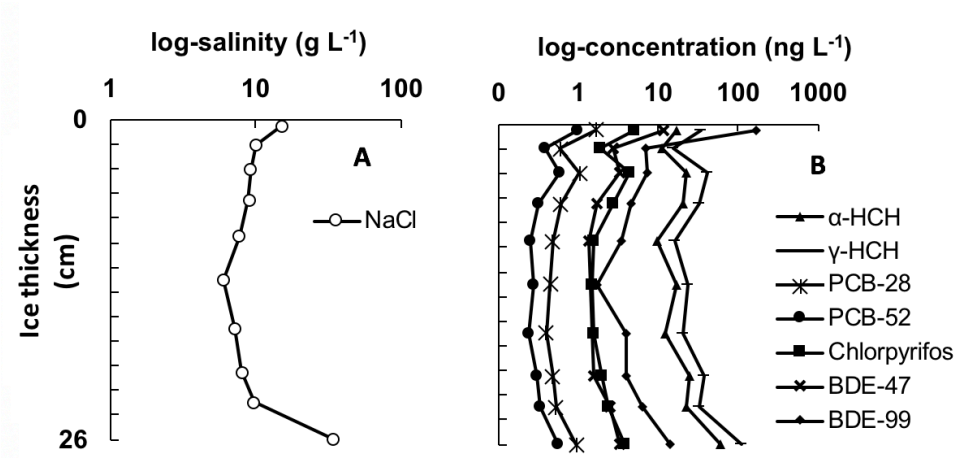

Figure 1: Chemical concentrations in a vertical section of sea ice grown at -18 ºC to a depth of 26cm. Zero on the y-axis represents the upper most surface of the ice in contact with the chamber atmosphere

We are confident that the NaCl profile provided in Figure 1 is driven by brine gravity drainage processes [23]. As the profiles for each organic chemical (Panel B) display a similar shape, we suggest that their distribution in young sea ice is strongly influenced by brine advection during ice growth.

313

314 3.4. Accumulation of POPs in frost flowers

315 Frost flowers (*FF*) are highly saline ice structures that develop on the surface of newly formed
316 sea ice, typically refreezing leads [27]. The salinity of frost flowers sampled in polar environments
317 have been measured up to 110 g L^{-1} (i.e. $EF_{FF\text{-}SW}$ = 3) [28] and are typically enriched in other
318 sea-salt ions as well [29, 30]. The leading mechanism proposed for this enrichment suggests that
319 freezing water vapour located at the sea ice surface forms an ice skeleton, causing salts and
320 other solutes to be advected from the surface layer through capillary action [29]. In our study,
321 frost flowers covered around 10% of the surface area of the ice (Freeze - 1) and melted
322 samples measured a salinity of 83 g L^{-1}, representing a significant enrichment of NaCl from
323 the upper layer layer ($EF_{FF\text{-}L1}$ = 5.0 ± <0.1). Results displayed in Table 3 show that $EF_{FF\text{-}L1\ [POPs]}$
324 > 1, indicating they too are advected with brine from the surface layer, but to a lesser degree.
325 However, chemical enrichment factors ($EF_{FF\text{-}L1}$) for BDE-47 and BDE-99 were 30 ± 20 and 50
326 ± 31, respectively, indicating selective fractionation of organic chemicals in frost flowers.
327 Douglas et al. [10] observed similar enrichments ($EF_{FF\text{-}L1}$ = 2 – 68) for a number of analogous
328 chemicals, including higher-chlorinated-PCBs, in frost flowers sampled on coastal sea ice
329 close to Barrow, Alaska.

330 The relatively large surface area of frost flowers has been suggested as an important
331 feature that enhances the atmospheric scavenging of airborne chemicals [10]. However,
332 atmospheric scavenging is unlikely to be significant in our experiments because the blanks
333 revealed negligible levels of the chemicals in the chamber air (Table S3). A possible
334 mechanism for observing enrichment in frost flowers involves evaporation of chemicals from
335 the relatively warmer surface ice layer, and subsequent condensation to the colder frost
336 flowers [10]. However, we propose that organic solutes may be advected from the ice at different
337 rates and related to factors controlled by their individual physicochemical properties. The high
338 enrichment observed for some of these chemicals suggests that frost flowers may play an
339 important role in the ice-atmosphere exchange of POPs in polar marine environments.

340

3.5. Simulated chemical behaviour in sea ice

The initial NaCl and chemical concentrations measured in the seawater were used as input parameters for the brine dynamics model. The model predicts the convection of brine, driven by gravity drainage, assuming that: (i) the chemicals are perfectly dissolved and are advected with the moving brine; (ii) the chemicals are well-mixed in the underlying seawater. Figure 2 shows an example of a comparision between the predicted and measured chemical distribution of NaCl (Panel A), α-HCH (Panel B) and BDE-47 (Panel C) (see Figures S3 and S4 for other chemical profiles), normalised by ice thickness. The model produced a predictable 'c-shape' concentration profile for NaCl and organic chemicals, where concentrations were generally highest at the upper and lower sea ice interface.

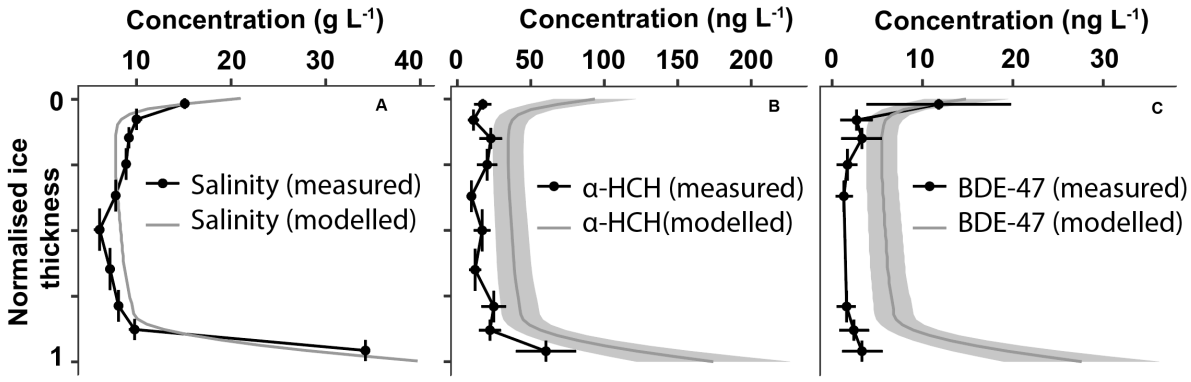

Figure 2: Modelled and measured bulk concentration profile for salinity, α-HCH and BDE-47 in sea ice grown at -18°C to a depth of 26 cm. Vertical bars indicate layer thickness. Horizontal bars represent ± 2 s.d. for modelled (grey shade) and measured data.

Although a qualitative comparison between the measured and modelled chemical profiles in the sea ice was reasonable, the model tended to overestimate the concentrations of the organic chemicals. A ratio of the modelled and measured bulk ice concentrations (integrated vertically over all the sea ice layers) showed a ratio for NaCl of around 1, whereas a ratio of 9 was observed for BDE-47 (see Table S6 for other chemicals). The comparison suggests that low-polarity organic compounds may not be transported conservatively with respect to salt. Rather, additional factors other than gravity drainage may also play a role in the degree of chemical incorporation during sea ice growth.

The extreme environment (i.e. low temperatures and high brine salinity) in sea ice causes large uncertainties regarding the physical-chemical properties of organic solutes in brine inclusions. We derived simple salinity-temperature dependent relationships for each chemical to estimate whether the aqueous solubility was exceeded at the minimum recorded temperature and highest modelled brine salinity within the sea ice (listed in Table 1). Our basic approach indicated that the aqueous solubility was not exceeded for each chemical at these

conditions. While we can not state conclusively that this factor did not affect the distribution of chemicals in our experiments, our results suggest that another process(es) currently not described by the physics incorporated within the brine dynamics model may also be at play. Given the dynamic nature of our artificial sea ice, chemical solutes are unlikely to attain equilibrium between the seawater, ice surfaces and ice brine compartments. As sea ice grows thicker (late season Arctic sea ice may be several metres thick), the rate of ice growth generally decreases, allowing more time for exchange of organic chemicals between these compartments and affecting their accumulation in sea ice. We therefore propose that thermodynamic factors such as the partitioning of low polarity organic contaminants between these different ice compartments [31] (processes which do not feature in the model) may account for the descrepancy between the observed and modelled values.

3.6. Brine composition and chemical dynamics

The thermodynamic state controls the fluid dynamics of sea ice and plays a crucial role in the biogeochemical cycling of sea ice constituents [8, 21, 32, 33]. As the brine volume of sea ice approaches around 5%, it is generally accepted that sea ice becomes sufficiently permeable to permit brine to move freely [34] . However, the melting of natural sea ice and hence its desalination during seasonal thaw is a complex process that is governed by the properties of the sea ice and the thermal regime (i.e. basal melt or surface melt). We conducted a slow-melt experiment (see section 2.4.) to investigate the association of organic chemicals with different meltwater fractions of varying NaCl concentrations. This enabled us to observe the composition of brine and therefore infer the temporal behaviour of organic contaminants in sea ice during the transition from FYI to older MYI.

The experiment resulted in brine-rich meltwater being released first (e.g. NaCl; MW_{F1} = 58 g L^{-1}), followed by a supply of fresher meltwater due to the melting of the ice-matrix itself (e.g. NaCl; MW_{F4}= 1.9 g L^{-1}), indicating that brine release is governed by thermodynamically controlled phase-changes within the sea ice pores. Figure S2 shows that the level of chemical enrichment in meltwater (i.e. $EF_{MW\text{-}SW}$) was positively correlated (n=48, r^2=0.507, $p<0.01$) with the concentration of NaCl in the sea ice meltwater. Therefore, saltier brine can be expected to contain higher concentrations of chemicals. Our results are consistent with field studies investigating inorganic [21, 32] and organic [8, 9] chemical behaviour in sea ice.

402 Despite earlier meltwater fractions showing a higher degree of chemical enrichment,
403 the volumes of meltwater that were collected varied from 0.2 to 2.4 L (see Table S7). To further
404 investigate the dynamics of chemicals during melt, the percentage mass of chemical in each
405 meltwater fraction was calculated (see Table S8) and shown in Figure 3. The results show
406 that the highest mass of the most hydrophobic chemicals (PCB-28, chlorpyrifos, BDE-47,
407 BDE-99) was present in the final meltwater fraction (MW_{F4}), unlike NaCl which has the lowest
408 mass in MW_{F4}. The results indicate that organic chemicals can be retained within the bulk sea
409 ice even after the brine has drained and implies that more hydrophobic chemicals are
410 preferentially retained within the sea ice.

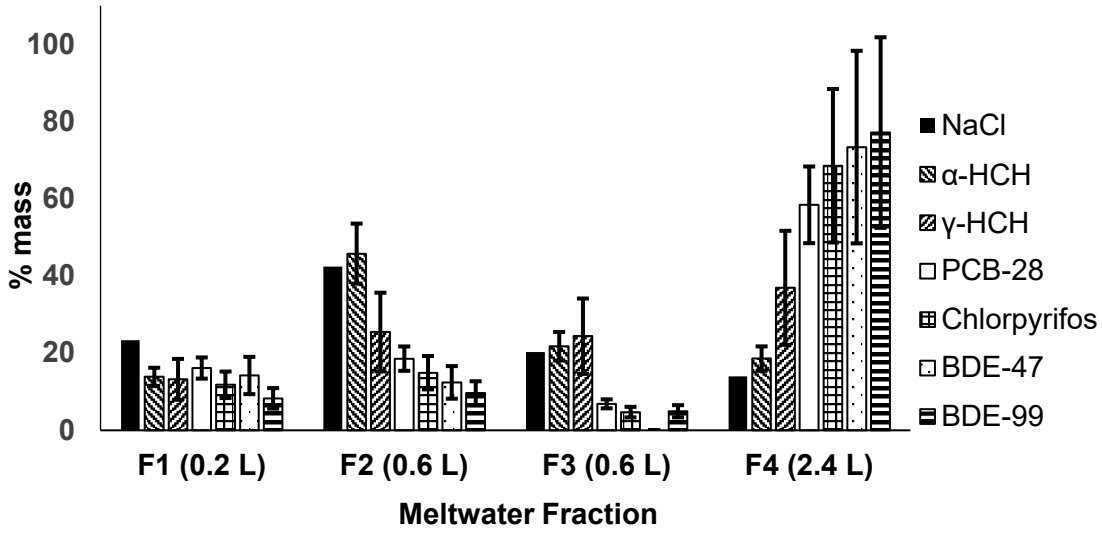

411 Figure 3: The percentage mass of individual chemicals in the sequential meltwater fractions.
412 Bracketed values are the actual volumes for each meltwater fraction. PCB-52 was <MDL in
413 several fractions and so was not included in this plot. Error bars calculated from RSD.
414
415 The three initial meltwater fractions (MW_{F1-F3}) show that chemical mass loss from the
416 ice is lower than salt, but highest for the more water soluble chemicals (i.e. around 75% of α-
417 HCH and γ-HCH is lost in F1 to F3, compared to only around 20% of BDE-99). The final melt
418 fraction (MW_{F4}) contained >50 % of the mass of (in increasing order) PCB-28, chlorpyrifos,
419 BDE-47 and BDE-99, initially present in the ice prior to the onset of melt. The results suggest
420 that chemicals are released at variable rates, possibly due to thermodynamic factors
421 associated with the aqueous solubility and the rate of dissolution [35], which may affect the
422 phase distribution and rate of transfer between the solid fresh ice matrix to the mobile liquid
423 brine solution. This observation is comparable to studies performed in environmental and
424 laboratory snow, whereby soluble ions are generally released in initial meltwater fractions (i.e.
425 "type I elution" see references [36, 37]), wheareas very hydrophobic organic compounds (possibly

associated with particles), are retained in the snow until final meltwater elution associated with complete melting (i.e. “type II elution”).

Our results show that brine dynamics play an important role in the distribution of persistent chemicals in young sea ice, supporting our hypothesis that chemical uptake and distribution is strongly influenced by the formation of brine during sea ice growth. However, chemical specific processes may remove these chemicals from the dissolved phase, decoupling them from the NaCl within the sea ice system. Support for this assertion comes from our melting experiments where chemicals were released from the sea ice at varying rates. The most hydrophobic chemicals were preferentially retained within the sea ice relative to the more water soluble chemicals, and to NaCl. Physical-chemical processes such as adsorption to brine inclusion walls or precipitation within brine inclusions are promising explanations for this behaviour. Our results have several important implications for the biogeochemical cycling of persistent organic pollutants in natural sea ice, by: (i) altering the input rate of different contaminants to surface waters from melting sea ice; (ii) affecting the level and retention rates of chemical contaminants in FYI and subsequent MYI, and; (iii) controlling the spatial and temporal exposure of chemicals to ice-associated biota.

Tables S1 – S7 show chemical data along with associated Equations S1 – S5 and Figures S1 – S4 which is available as Supporting Information (SI) to this manuscript.

Acknowledgements

JG’s PhD (NE/L002604/1) was funded through NERC’s ENVISION Doctoral Training Centre. This work resulted from the EISPAC project (NE/R012857/1), part of the Changing Arctic Ocean programme, jointly funded by the UKRI Natural Environment Research Council (NERC) and the German Federal Ministry of Education and Research (BMBF). The authors are grateful to the British Antarctic Survey for providing funding (British Antarctic Survey Collaboration Voucher) to cover the running costs of the RvG-ASIC facility for the duration of the experimental period. This project/work has received funding from the European Union’s Horizon 2020 research and innovation programme through the EUROCHAMP-2020 Infrastructure Activity under grant agreement No 730997. The authors would like to thank Professor Finlo Cottier and two other anonymous reviewers.

1. UNEP *Global Report 2003-Regionally Based Assessment of Persistent Toxic Substances*; Geneva, Switzerland, 2003.https://www.researchgate.net/profile/Hindrik_Bouwman/publication/292286858_Regionally_based_assessment_of_persistent_toxic_substances_Global_reprt/links/56ac8fb408ae19a38513e2e7/Regionally-based-assessment-of-persistent-toxic-substances-Global-reprt.pdf
2. de Wit, C. A.; Muir, D., Levels and trends of new contaminants, temporal trends of legacy contaminants and effects of contaminants in the Arctic: Preface. *Science of the Total Environment* **2010,** *408* (15), 2852-2853;10.1016/j.scitotenv.2009.06.011
3. AMAP *AMAP Assessment 2016: Chemicals of Emerging Arctic Concern*; -; -: Oslo, Norway, -, 2017; p 353.https://www.amap.no/documents/doc/AMAP-Assessment-2016-Chemicals-of-Emerging-Arctic-Concern/1624
4. Cai, M.; Yang, H.; Xie, Z.; Zhao, Z.; Wang, F.; Lu, Z.; Sturm, R.; Ebinghaus, R., Per- and polyfluoroalkyl substances in snow, lake, surface runoff water and coastal seawater in Fildes Peninsula, King George Island, Antarctica. *Journal of Hazardous Materials* **2012,** *209-210*, 335-342;10.1016/j.jhazmat.2012.01.030
5. Pućko, M.; Stern, G. A.; Macdonald, R. W.; Rosenberg, B.; Barber, D. G., The influence of the atmosphere-snow-ice-ocean interactions on the levels of hexachlorocyclohexanes in the Arctic cryosphere. *Journal of Geophysical Research: Oceans* **2011,** *116* (C2), n/a-n/a;10.1029/2010JC006614
6. Pućko, M.; Stern, G. A.; Macdonald, R. W.; Jantunen, L. M.; Bidleman, T. F.; Wong, F.; Barber, D. G.; Rysgaard, S., The delivery of organic contaminants to the Arctic food web: Why sea ice matters. *Science of the Total Environment* **2015,** *506-507*, 444-452;10.1016/j.scitotenv.2014.11.040
7. Gustafsson, Ö.; Andersson, P.; Axelman, J.; Bucheli, T. D.; Kömp, P.; McLachlan, M. S.; Sobek, A.; Thörngren, J. O., Observations of the PCB distribution within and in-between ice, snow, ice-rafted debris, ice-interstitial water, and seawater in the Barents Sea marginal ice zone and the North Pole area. *Science of the Total Environment* **2005,** *342* (1), 261-279;10.1016/j.scitotenv.2004.12.044
8. Pućko, M.; Stern, G.; Macdonald, R. W.; Barber, D. G., alpha- and gamma-Hexachlorocyclohexane Measurements in the Brine Fraction of Sea Ice in the Canadian High Arctic Using a Sump-Hole Technique. *Environmental Science & Technology* **2010,** *44* (24), 9258-9264;10.1021/es102275b
9. Pućko, M.; Stern, G. A.; Barber, D. G.; Macdonald, R. W.; Rosenberg, B., The international polar year (IPY) circumpolar flaw lead (CFL) system study: The importance of brine processes for α- and γ-hexachlorocyclohexane (HCH) accumulation or rejection in sea ice. *Atmosphere-Ocean* **2010,** *48* (4), 244-262;10.3137/OC318.2010
10. Douglas, T. A.; Domine, F.; Barret, M.; Anastasio, C.; Beine, H. J.; Bottenheim, J.; Grannas, A.; Houdier, S.; Netcheva, S.; Rowland, G.; Staebler, R.; Steffen, A., Frost flowers growing in the Arctic ocean-atmosphere–sea ice–snow interface: 1. Chemical composition. *Journal of Geophysical Research: Atmospheres* **2012,** *117* (D14), n/a-n/a;10.1029/2011JD016460
11. Vaughan, D. G. C., J.C.; Allison, I.; Carrasco, J.; Kaser, G.; Kwok, R.; Mote, P.; Murray, T.; Paul, F.; Ren, J.; Rignot, E.; Solomina, O.; Steffen, K.; Zhang, T., Observations: Cryosphere. In *Climate Change 2013: The Physical Science Basis. Contribution of Working Group I to the Fifth Assessment Report of the Intergovernmental Panel on Climate Change*, Cambridge University: Cambridge, U.K. & New York, USA., 2013.

12. NSIDC All About Sea Ice: Arctic vs. Antarctic. https://nsidc.org/cryosphere/seaice/characteristics/difference.html

13. Perovich, D. M., W; Tschudi, M; Farrel, S. ; Hendricks, S; Gerland, S; Haas, C; Krumpen, T; Polashenski, C; Ricker, R; Webster, M Sea Ice. In: Arctic Report Card 2015. https://www.arctic.noaa.gov/report-card

14. Notz, D.; Worster, M. G., Desalination processes of sea ice revisited. *Journal of Geophysical Research: Oceans* **2009,** *114* (C5), n/a-n/a;10.1029/2008JC004885

15. Pućko, M.; Stern, G. A.; Barber, D. G.; Macdonald, R. W.; Warner, K. A.; Fuchs, C., Mechanisms and implications of α-HCH enrichment in melt pond water on Arctic sea ice. *Environmental Science & Technology* **2012,** *46* (21), 11862;10.1021/es303039f

16. Pućko, M.; Stern, G. A.; Burt, A. E.; Jantunen, L. M.; Bidleman, T. F.; Macdonald, R. W.; Barber, D. G.; Geilfus, N.-X.; Rysgaard, S., Current use pesticide and legacy organochlorine pesticide dynamics at the ocean-sea ice-atmosphere interface in resolute passage, Canadian Arctic, during winter-summer transition. *Science of the Total Environment* **2017,** *580*, 1460-1469;10.1016/j.scitotenv.2016.12.122

17. Rees Jones, D. W.; Worster, M. G., A physically based parameterization of gravity drainage for sea-ice modeling. *Journal of Geophysical Research: Oceans* **2014,** *119* (9), 5599-5621;10.1002/2013JC009296

18. Cottier, F.; Eicken, H.; Wadhams, P., Linkages between salinity and brine channel distribution in young sea ice. *Journal of Geophysical Research: Oceans* **1999,** *104* (C7), 15859-15871;10.1029/1999JC900128

19. Fripiat, F.; Cardinal, D.; Tison, J. L.; Worby, A.; André, L., Diatom-induced silicon isotopic fractionation in Antarctic sea ice. *Journal of Geophysical Research: Biogeosciences* **2007,** *112* (G2), n/a-n/a;10.1029/2006JG000244

20. Nomura, D.; Takatsuka, T.; Ishikawa, M.; Kawamura, T.; Shirasawa, K.; Yoshikawa-Inoue, H., Transport of chemical components in sea ice and under-ice water during melting in the seasonally ice-covered Saroma-ko Lagoon, Hokkaido, Japan. *Estuarine, Coastal and Shelf Science* **2009,** *81* (2), 201-209;10.1016/j.ecss.2008.10.012

21. Fripiat, F.; Sigman, D. M.; Fawcett, S. E.; Rafter, P. A.; Weigand, M. A.; Tison, J. L., New insights into sea ice nitrogen biogeochemical dynamics from the nitrogen isotopes. *Global Biogeochemical Cycles* **2014,** *28* (2), 115-130;10.1002/2013GB004729

22. Miller, L. A. F., F; Brent, G. T. Else; Bowman, J S; Brown, K A; Collins, E R; Ewert, M; Fransson, A; Gosselin, M; Lannuzel, D; Meiners, K M; Michel, C; Nishioka, J; Nomura, D; Papadimitriou, S; Russell, L M; Sørensen, L L; Thomas, D N; Tison, J-L; A. van Leeuwe, M; Vancoppenolle, M; Wolff, E W; Zhou, J, Methods for biogeochemical studies of sea ice: The state of the art, caveats, and recommendations. *Elementa: Science of the Anthropocene* **2015,** *3*;10.12952/journal.elementa.000038

23. Thomas, M. Brine and pressure dynamics in growing sea ice: first results from the Roland von Glasow air-sea-ice chamber. Ph.D, University of East Anglia, Norwich, U.K., 2019.

24. Thomas, M. V., M; France, J; Sturges, W. T. ; D. C. E. Bakker, D. C. E. ; Kaiser, J.; von Glasow, R, Tracer measurements in growing sea ice support convective gravity drainage parameterisations (Ph.D Thesis). 2019.

25. Petrich, C. E., Hajo, Overview of sea ice growth and properties. In *Sea ice (Third Edition)*, Third ed.; John Wiley & Sons: Chichester, U.K., 2017; pp 1-41.

26. Assur, A., Composition of sea ice and its tensile strength, in Arctic Sea Ice. Easton, M., Ed. National Research Council, Washington: Easton, Maryland, 1958; pp 106 - 138.

27. Perovich, D. K.; Richter-Menge, J. A., Surface characteristics of lead ice. *Journal of Geophysical Research: Oceans* **1994,** *99* (C8), 16341-16350;10.1029/94JC01194

28. Barber, D. G. E., J K ; Pućko, M ; Rysgaard, S ; Deming, J W ; Bowman, JS ; Papakyriakou, T ; Galley, R J ; Sogaard, D H, Frost flowers on young Arctic sea ice: The climatic, chemical, and microbial significance of an emerging ice type. *Journal Of Geophysical Research-Atmospheres* **2014,** *119* (20), 11593-11612

29. Alvarez-Aviles, L.; Simpson, W. R.; Douglas, T. A.; Sturm, M.; Perovich, D.; Domine, F., Frost flower chemical composition during growth and its implications for aerosol production and bromine activation. *Journal of Geophysical Research: Atmospheres* **2008,** *113* (D21), n/a-n/a;10.1029/2008JD010277

30. Rankin, A. M.; Wolff, E. W.; Martin, S., Frost flowers: Implications for tropospheric chemistry and ice core interpretation. *Journal of Geophysical Research: Atmospheres* **2002,** *107* (D23), AAC 4-1-AAC 4-15;10.1029/2002JD002492

31. Schwarzenbach, R. P. G., Phillip M; Imboden, Dieter M, Sorption of Nonionic organic compounds to Inorganic Surfaces in Water. In *Environmental Organic Chemistry*, John Wiley & Sons: Hoboken, New Jersey, 2003; pp 389 - 417.

32. Lannuzel, D.; Bowie, A. R.; van Der Merwe, P. C.; Townsend, A. T.; Schoemann, V., Distribution of dissolved and particulate metals in Antarctic sea ice. *Marine Chemistry* **2011,** *124* (1), 134-146;10.1016/j.marchem.2011.01.004

33. Zhou, J.; Delille, B.; Kaartokallio, H.; Kattner, G.; Kuosa, H.; Tison, J. L.; Autio, R.; Dieckmann, G. S.; Evers, K. U.; Jørgensen, L.; Kennedy, H.; Kotovitch, M.; Luhtanen, A. M.; Stedmon, C. A.; Thomas, D. N., Physical and bacterial controls on inorganic nutrients and dissolved organic carbon during a sea ice growth and decay experiment. *Marine Chemistry* **2014,** *166* (C), 59-69;10.1016/j.marchem.2014.09.013

34. Golden; Ackley; Lytle, The percolation phase transition in sea Ice. *Science (New York, N.Y.)* **1998,** *282* (5397), 2238;10.1126/science.282.5397.2238

35. Schwarzenbach, R. P. G., Phillip M; Imboden, Dieter M, Molecular interpretation of the Excess Free Energy of Organic Compounds in Aqueous Solutions. In *Environmental Organic Chemistry*, John Wiley & Sons: Hoboken, New Jersey, 2003; pp 142 - 180.

36. Meyer, T.; Lei, Y.; Muradi, I.; Wania, F., Organic Contaminant Release from Melting Snow. 2. Influence of Snow Pack and Melt Characteristics. *Environmental Science & Technology* **2009,** *43* (3), 663;10.1021/es8020233

37. Meyer, T.; Lei, Y.; Muradi, I.; Wania, F., Organic Contaminant Release from Melting Snow. 1. Influence of Chemical Partitioning. *Environmental Science & Technology* **2009,** *43* (3), 657;10.1021/es8020217

Jack Garnett[1], Crispin Halsall[1*], Max Thomas[2], James France[2,3,4], Jan Kaiser[2], Carola Graf[1], Amber Leeson[1], Peter Wynn[1]

1 Lancaster Environment Centre, Lancaster University, Lancaster, LA1 4YQ, UK
2 Centre for Ocean and Atmospheric Sciences, School of Environmental Sciences, University of East Anglia, Norwich Research Park, Norwich, NR4 7TJ, UK
3 British Antarctic Survey, High Cross, Madingley Road, Cambridge, CB3 0ET
4 Department of Earth Sciences, Royal Holloway, University of London, Egham Hill, Egham TW20 0EX, UK
*Corresponding author: c.halsall@lancaster.ac.uk

Supporting Information to:

Mechanistic insight into the uptake and fate of persistent organic pollutants in sea ice

Contents include:

18 pages (S1-S18)
Tables (S1-S7)
Equations (S1-S5)
Figures (S1-S4)
Further information

Tables

Table S1: Physical-chemical property data for organic chemicals.

Chemical	Molar mass [g/mol]	Aqueous Solubility (nM) [25 °C]	Salinity & Temperature adjusted aqueous solubility [-2 °C] (nM)	Vapour pressure (Pa) [25°C]	Log Kow	References
α - HCH	290.9	3.33×10^{5}	1.68×10^{5}	2.45×10^{-1}	3.9	[1]
γ - HCH	290.9	2.47×10^{5}	9.36×10^{4}	7.59×10^{-2}	3.8	[1]
§Chlorpyrifos	350.6	9.95×10^{3}	2.19×10^{3}	3.10×10^{-3}	5.1	[2]
PCB-28	257.5	6.64×10^{3}	2.26×10^{2}	2.69×10^{-2}	5.7	[3]
PCB-52	292.0	6.50×10^{2}	1.23×10^{2}	1.20×10^{-2}	5.9	[3]
*BDE-47	485.8	3.43×10^{2}	1.02×10^{2}	2.15×10^{-4}	6.4	[4]
*BDE-99	564.7	1.95×10^{2}	3.98×10^{1}	3.63×10^{-5}	6.8	[4]

Aqueous solubility data are reported for 25°C but were adjusted to the freezing temperature of seawater (-2°C) and initial seawater salinity (35.4 g L^{-1}) (see Equation S2) to estimate solubility. Temperature and salinity adjustments were calculated independently using temperature-dependent regression parameters provided in the corresponding references. § denotes those chemicals for which temperature regression parameters were not available. Salinity adjustments were performed using predicted Setchenow constants[5] .

38

39 Table S2: Concentrations of chemical spike added into experimental tank

40

Compound	Volume (L)	Molarity (μM)	Volume (L)	Molarity (nM)
	Spike*		Experiment tank	
α-HCH	1	1.43	3500	0.41
γ-HCH		1.43		0.41
PCB-28		1.21		0.35
PCB-52		0.43		0.12
Chlorpyrifos		1.02		0.29
BDE-47		0.21		0.06
BDE-99		0.74		0.21

41

42 *The mixed-stock chemical solution was made up with 1 litre of pure ethanol giving a final volume fraction in the experimental tank of

43 approximately 3 x 10^{-4}.

Table S3: QA/QC parameters used throughout experiment

Chemical	*α -HCH*	*γ -HCH*	*PCB-28*	*PCB-52*	*Chlorpyrifos**	*BDE-47*	*BDE-99*
Units	*ng* L^{-1}	*ng* L^{-1}	*ng* L^{-1}	*ng* L^{-1}	*ng* L^{-1}	*ng* L^{-1}	*ng* L^{-1}
**SW Procedural blank (n=3)*	*n/d*	*n/d*	*n/d*	*n/d*	*n/d*	*n/d*	*2 ± 4*
**BI Procedural blank (n=1)*	*<3*	*<3*	*<0.1*	*<0.1*	*n/d*	*n/d*	*n/d*
Method Detection limit (MDL)	*<5*	*<15*	*<0.3*	*<0.3*	*<13*	*<0.3*	*<13*
Recovery Standard	*^{13}C-PCB-28*			*^{13}C-PCB-52*		*^{13}C-PCB-180*	
Internal Standard	*^{13}C-PCB-141*					*BDE-69*	
BI (% recovery)	*38 ± 12*			*42 ± 14*	*42 ± 15*		
SW (% recovery)	*34 ± 11*			*45 ± 12*	*38 ± 19*		
Maximum seawater RSD	17	40	8	13	24	34	32

MDL calculated using SW (*n* = 3) & BI (*n* = 1) procedural blanks; n/d=not detected; *Confirmation ions for chlorpyrifos were not always detected in some samples containing low analyte levels. The maximum relative standard deviation in the seawater measurements was used to provide a conservative estimate of the variability for some singlet samples.

Table S4: Values used for calculations for literature analysis

Experimental compartment	NaCl	α -HCH	γ -HCH	PCB-28	PCB-52	Chlorpyrifos	BDE-47	BDE-99	Experiment
	g L^{-1}	ng L^{-1}	ng L^{-1}	ng L^{-1}	ng L^{-1}	ng L^{-1}	ng L^{-1}	ng L^{-1}	
Brine	53.1	107.7	278.1	31.1	10.3	63.5	21.4	60.5	Freeze 2
SW	37.9	185.6	336.3	24.9	8.5	58.0	36.9	73.8	Freeze 1
BI	13.9	25.4	39.8	4.6	1.3	8.5	4.7	23.7	Freeze 1
BI	11.1	31.0	73.6	5.5	0.7	15.6	5.0	25.3	Freeze 2
FF	88.3	35.6	66.6	4.9	3.3	17.9	208.7	1555.7	Freeze 1
L1	17.6	24.1	42.2	2.1	1.1	8.4	8.1	36.1	Freeze 1

Table S5: Modelled and measured integrated concentrations of chemicals in bulk ice.

	NaCl	α-HCH	γ-HCH	PCB-28	PCB-52	Chlorpyrifos	BDE-47	BDE-99	Experiment
Modelled	12.3	54.9	125.8	7.0	2.8	17.7	8.7	21.4	Freeze 1
Measured	13.7	16.0	25.5	1.3	0.8	5.2	1.0	15.1	
Modelled:Measured	0.9	3.4	4.9	5.3	3.5	3.4	8.6	1.4	
Modelled	10.7	47.6	109.2	6.1	2.4	15.3	7.6	18.6	Freeze 2
Measured	13.7	16.0	25.5	1.3	0.8	5.2	1.0	15.1	
Modelled:Measured	0.8	3.0	4.3	4.6	3.1	3.0	7.5	1.2	

Table S6: Concentration of chemicals in meltwater fractions and Enrichment Factor (EF).

MW	H_20	NaCl		α -HCH		γ -HCH		PCB-28		PCB-52		Chlorpyrifos		BDE-47		BDE-99	
	L	g L^{-1}	EF	ng L^{-1}	EF	ng L^{-1}	EF	ng L^{-1}	EF	ng L^{-1}	EF	ng L^{-1}	EF	ng L^{-1}	EF	ng L^{-1}	EF
F1B	0.10	48.3	1.27	109.7	0.59	303.2	0.90	25.2	1.01	10.2	1.21	47.0	0.81	22.7	0.61	53.8	0.73
F1T	0.09	57.9	1.53	105.7	0.57	253.0	0.75	36.9	1.48	10.4	1.23	80.0	1.38	20.2	0.55	67.3	0.91
F2B	0.36	30.1	0.79	122.5	0.66	174.6	0.52	7.9	0.32	<MDL	n/a	11.0	0.19	<MDL	n/a	14.0	0.19
F2T	0.24	31.0	0.82	98.2	0.53	164.3	0.49	16.1	0.65	5.8	0.68	46.2	0.80	14.9	0.40	34.3	0.46
F3B	0.31	12.8	0.34	46.7	0.25	178.4	0.53	2.0	0.08	<MDL	n/a	6.8	0.12	<MDL	n/a	12.9	0.17
F3T	0.28	16.6	0.44	62.2	0.34	148.7	0.44	6.6	0.26	<MDL	n/a	9.3	0.16	<MDL	n/a	9.8	0.13
F4B	1.07	1.9	0.05	13.3	0.07	67.6	0.20	5.3	0.21	<MDL	n/a	20.0	0.34	5.2	0.14	7.1	0.10
F4T	1.30	3.1	0.08	10.2	0.05	58.5	0.17	11.9	0.48	<MDL	n/a	36.8	0.63	11.9	0.32	76.2	1.03

Meltwater was successively collected from the top (T) and bottom (B) sections of the ice samples from Freeze 2 (Fraction 1=F1; Fraction 2=F2; Fraction 3=F3; Fraction 4=F4). <MDL=below method detection limit; n/a=not applicable

Table S7: Percentage mass of chemicals in meltwater fractions.

Fraction Name (Volume (L))	H_20	NaCl	α -HCH	γ -HCH	PCB-28	PCB-52*	Chlorpyrifos	BDE-47	BDE-99
	$\%_{volume}$	$\%_{mass}$	$\%_{mass}$	$\%_{mass}$	$\%_{mass}$	$\%_{mass}$	$\%_{mass}$	$\%_{mass}$	$\%_{mass}$
F1 (0.2 L)	5	23	13.9	13.2	16.1	n/c	11.8	14.2	8.3
F2 (0.6 L)	16	42	45.8	25.5	18.6	n/c	14.9	12.4	9.6
F3 (0.6 L)	16	20	21.8	24.4	6.9	n/c	4.7	0.0	4.9
F4 (2.4 L)	63	14	18.6	36.9	58.4	n/c	68.5	73.4	77.1

The volume of water and the mass of each chemical from the respective meltwater fractions (Fraction 1=F1; Fraction 2=F2; Fraction 3=F3; Fraction 4=F4) obtained from the top (T) and bottom (B) were summed (e.g. F1T + F1B) and the % mass contribution was calculated. *PCB-52 was <MDL in some meltwater fractions and so was excluded from further data analysis; n/c=not calculated

Equations

Equation S1: Brine salinity

$$S_{br} = -17.6T - 0.389^2 - 0.00362T^3 \quad (1)$$

Brine salinity in sea-ice (g kg^{-1}) is a function of temperature because, to an excellent approximation, the salinity of brine remains in thermodynamic equilibrium as water freezes or melts at brine pocket walls (Feltham et al. 2006). Brine salinity is derived from the experimental data [6, 7].

Equation S2: Salinity & Temperature-adjusted aqueous solubility (S^T)

$$\log(S^T/S_0^T) = (-k_{salt}\, C_{salt}) \qquad (2)$$

Where k_{salt} is the Setschenow constant derived using k = 0.04Kow + 0.114 [5]; Kow = octanol-water partition coefficient; C_{salt} is the molar concentration of NaCl; S^T and S_0^T are the aqueous solubilities of the organic solute in aqueous salt solution and in water, respectively, at a particular temperature using temperature-dependent regression curves. See references for physical-chemical data. All units of concentration and solubility are Molarity.

Equation S3: Normalised ice depth

$$Normalised\ depth = \frac{ice\ layer\ depth \quad (e.g.13cm)}{Total\ ice\ thickness\ (e.g.26cm)} \qquad (3)$$

Due to differences in ice thickness between the modelled and measured ice depths, ice thicknesses were normalised to allow comparison of the sea ice datasets.

Equation S4: Bulk ice concentration

$$[chemical]_{bulk\ ice}\ [ng\ L^{-1}] = \frac{\sum(concentration\ x\ depth)}{Total\ ice\ thickness} \qquad (4)$$

Chemical concentration in bulk ice was calculated by totalling the amount of chemical at each layer, over the total average ice thickness. Measured concentrations in melted bulk ice samples were previously corrected for ice density using previously determined estimates of 0.95 kg L^{-1}.

Equation S5: Percentage mass

$$Percentage\ mass\ (\%) = \frac{((chemical)_{mass\ e.g.\ F1,\ F2,\ F3,\ F4,})}{Mass\ \Sigma_{(F1-F4)}}\ x\ 100 \qquad (5)$$

Where (%) is the relative mass of chemical in a particular meltwater fraction compared to the combined mass contained in the meltwater fractions.

Figures

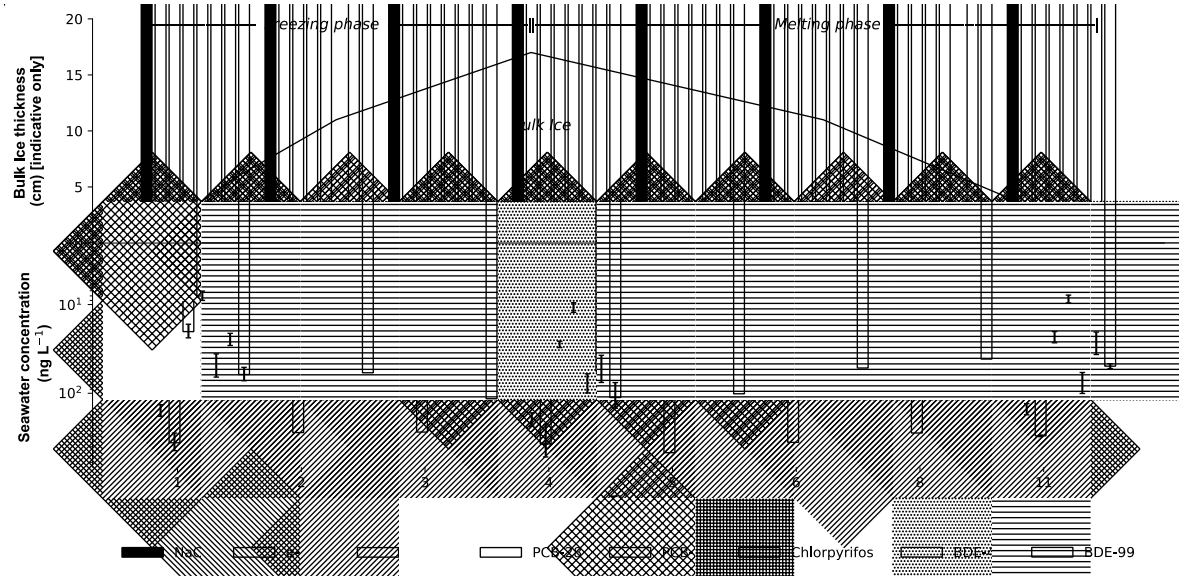

Figure S1: Time-series of NaCl and chemical concentrations in seawater.

Data were plotted on a log-scale to show all chemicals and account for their wide range in concentrations. Error bars indicate the 1.s.d on day 1, day 4 and day 11. The units of NaCl are g L^{-1}.

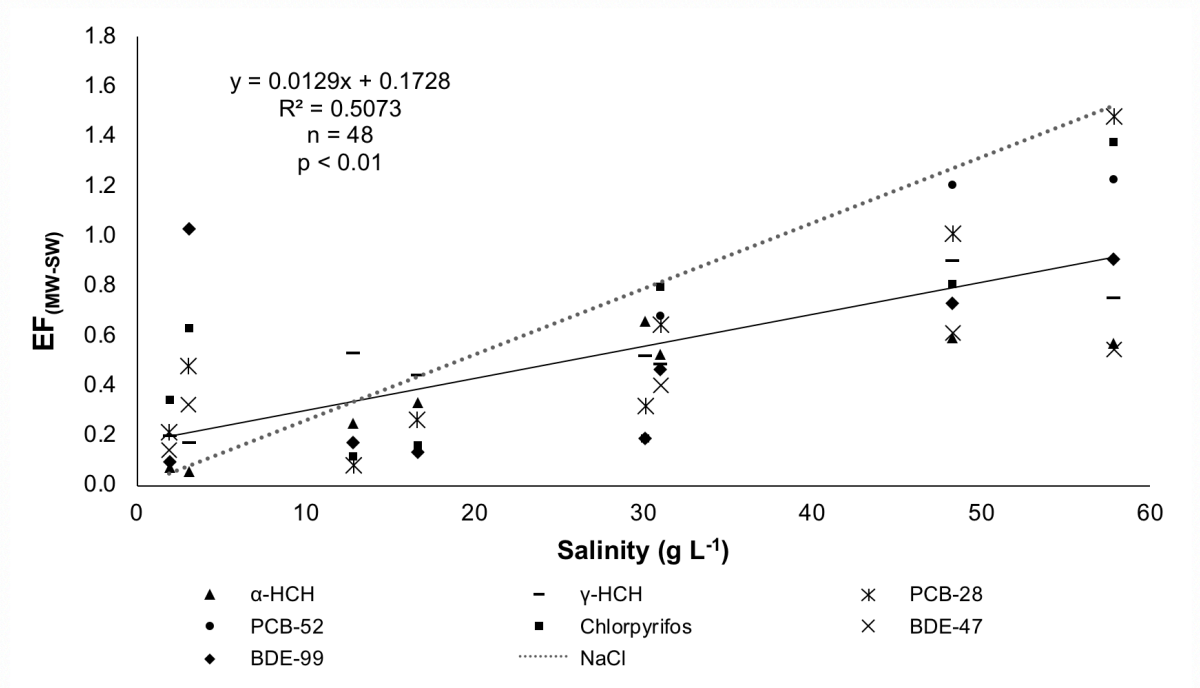

Figure S2: Relationship between the salinity and the level of chemical enrichment.

Symbols represent enrichment (EF_{MW-SW}) individual chemicals in the different meltwater fractions. Hashed line shows the enrichment of NaCl as a reference to compare chemical behaviour.

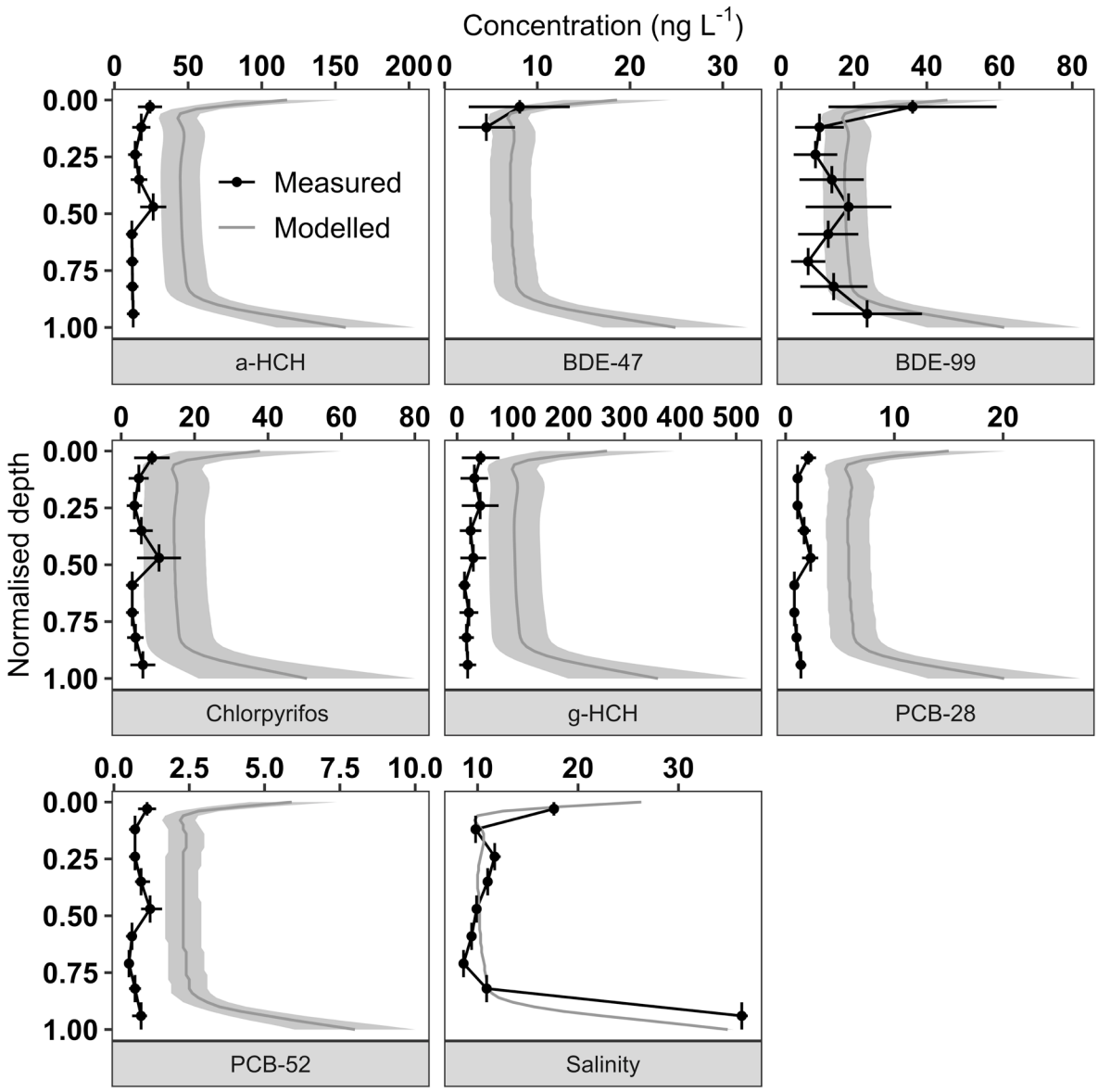

Figure S3: Chemical concentration profiles in sea ice grown during Freeze 1.

The salinity is in g L-1 rather than ng L-1.

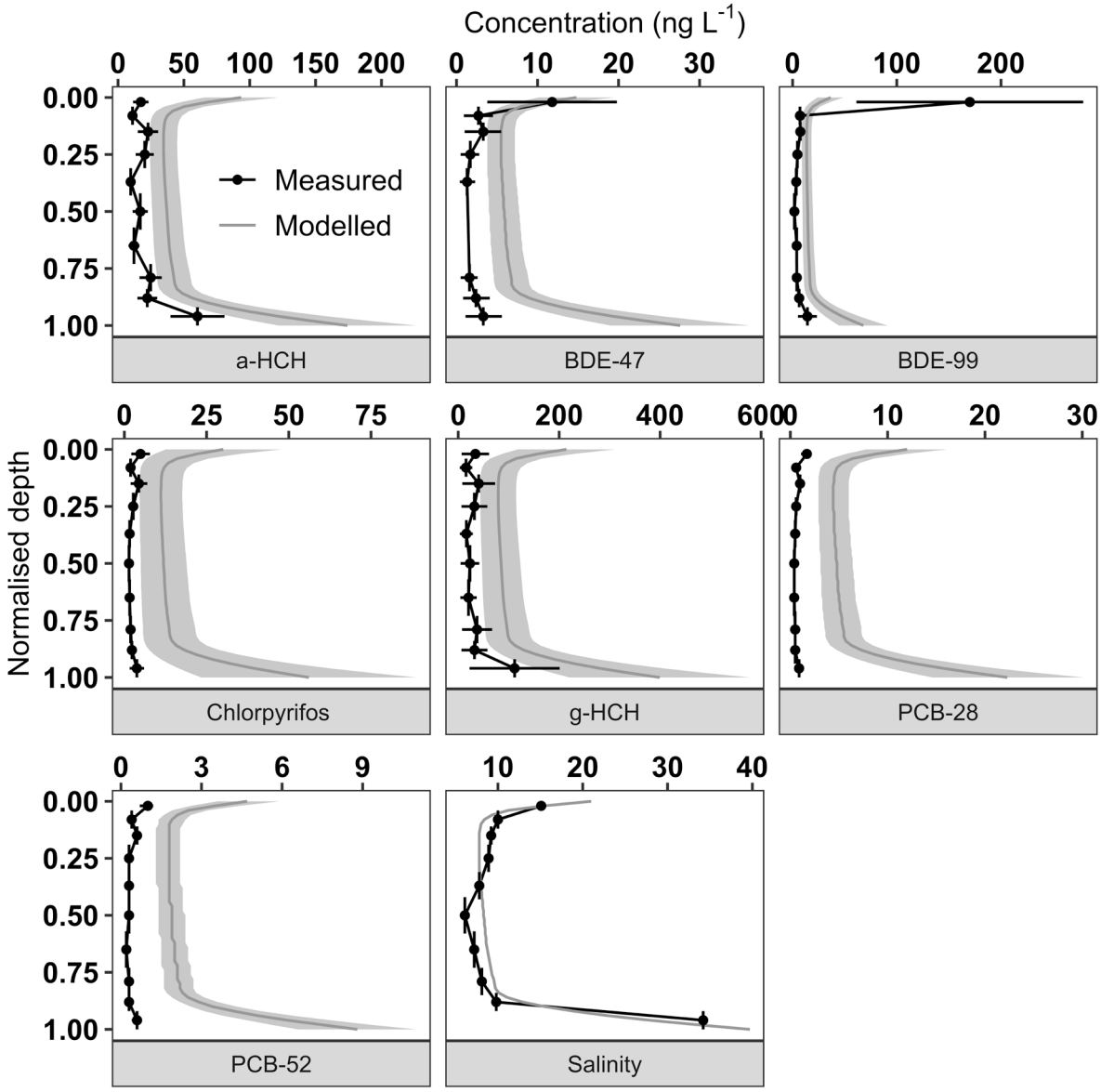

Figure S4: Chemical concentration profiles in sea ice grown during Freeze 2.

Salinity is in g L-1 rather than ng L-1.

Further information

1-dimensional sea ice brine dynamics model

The model used in this work is presented and evaluated in detail [8] Measured vertical sea ice temperature profiles, and sea-ice thicknesses derived from them, were used in lieu of modelled thermodynamics. The only processes affecting the concentrations of chemicals and salt within the model are the growth of new sea ice, which traps all of the dissolved species in the model, and gravity drainage. We parameterise gravity drainage following the well tested scheme [9]. The following describes the key steps in the model, and we re-direct the readers requiring more detail to [8].

During each model timestep, the brine salinity, S_{BR} (g kg^{-1}), is calculated from the local sea-ice temperature, T (ºC), using an inversion of the liquidus relationship for freezing NaCl (see Equation S1)

We then use the bulk salinity to calculate ϕ_l for each model layer using Equation S6:

$$\phi_l = \frac{S_b}{S_{br}} \qquad (6)$$

which is a rearrangement of the definition of bulk salinity assuming brine and ice are the only phases. The brine concentration, C_{br}, of any other chemical is calculated using Equation S7:

$$C_{br} = \frac{C_b}{\phi_l} \qquad (7)$$

where C_b is the bulk concentration of a chemical in the sea ice. The concentration of chemicals other than salt does not affect the physical sea-ice properties. From this point in the model there is no difference between the treatment of the transport of salt and any other chemical. To avoid duplicating equations we use C to represent salt and any other chemical from this point onwards.

Brine dynamics in the model are driven exclusively by gravity drainage [9]. The vertical brine salinity profile is always negative (highest brine salinities near the sea-ice/atmosphere interface) because of the negative temperature profile in growing sea ice (Equation S1). Brine density is proportional to brine salinity [10], so the brine density profile in growing sea ice is also negative. Relatively dense brine overlies less dense brine and ocean. This unstable brine

profile can cause convective overturning of brine, a process often referred to as 'gravity drainage'. Brine travels downwards through brine channels to the ocean, and is replaced by upwelling brine travelling through the porous sea-ice matrix. Dissolved chemical species are transported along with this brine, causing a net desalination of the sea ice and a redistribution of other chemicals. Gravity drainage is the dominant process redistributing brine in growing sea ice [6].

We parameterise gravity drainage [9] and note that the parameterisation of Griewank & Notz [11] is basically equivalent and performs equally well [8]. We evolve the concentration profile of salt and tracer using Equation S8:

$$\frac{dC_b}{dt} = -w\frac{dC_{br}}{dz} \qquad (8)$$

where t and z represent time and depth, respectively. Rees Jones & Worster [9] parameterise the upward brine velocity, w, as proportional to an effective Rayleigh number, R_e, using Equation S9:

$$w(z) = \begin{cases} -\alpha R_e \frac{k_l}{c_l}\frac{z-z_c}{(h-z_c)^2}, & z \geq z_c \\ 0, & otherwise \end{cases} \qquad (9)$$

where α is a free tuning parameter, k_l and c_l are the thermal conductivity and volumetric heat capacity of brine, respectively, and z_c and z are the depth of the convecting layer and the depth of the model layer, respectively. The depth of the convecting layer is taken to be the shallowest depth where the local Rayleigh number, $R(z)$, is greater that some critical Rayleigh number, R_c, which is a free tuning parameter. We use the formulation of Rees Jones & Worster [9] to calculate $R(z)$ for each model layer, then calculate R_e as a function of the maximum super critical Rayleigh number using Equation S10.

$$R_e = \max(R(z) - R_c) \qquad (10)$$

Rayleigh numbers have been used extensively to diagnose and parameterise sea-ice brine convection [9, 11, 12]. A Rayleigh number represents the ratio of the timescale over which a brine parcel descends to the timescale over which that parcel comes into thermal equilibrium with its surroundings. See Worster & Rees Jones [13] for a detailed discussion of Rayleigh numbers in sea ice.

Sea ice growth (change in thickness, dh) was calculated using Equation S11:

$$dh = h_i - h_{i-1} \quad (11)$$

where i denotes the model timestep. The new thickness of sea ice is taken to have the same concentration as the sea water for each chemical species; consistent with measurements of a continuous salinity profile during Arctic sea ice growth [14], and our current best understanding of brine dynamics. After sea ice growth, the concentration of the chemical species in the sea water (C_o) was determined using a discrete mass balance approach using Equations S12 – S14:

$$mC_{o,i} = mC_{o,i-1} - (mC_{si,i} - mC_{si,i-1}) \quad (12)$$

$$m_{o,i} = m_{o,i-1} - (m_{si,i} - m_{si,i-1}) \quad (13)$$

$$C_{o,i} = \frac{mC_{o,i}}{m_{o,i}} \quad (14)$$

In Equations S12 - S14, the updated mass of some chemical in the seawater , $mC_{o,i}$, is equal to the mass of that chemical in the seawater at the previous timestep, $mC_{o,i-1}$, minus the change in mass of that chemical in the sea ice, mC_{si}, after desalination and sea ice growth. The updated mass of ocean, $m_{o,i}$, is calculated in a similar fashion, using the change in sea ice mass, m_{si}. The updated seawater concentration, $C_{o,i}$, is then the updated mass of chemical in the seawater divided by the mass of ocean. The seawater is assumed to be perfectly mixed. At the end of each timestep, the model predicts the vertically-resolved bulk ice and brine concentrations, and well-mixed concentrations in seawater for any perfectly dissolved chemical species in the ocean/sea ice system.

Supporting References

1. Xiao, H.; Li, N.; Wania, F., Compilation, evaluation, and selection of physical-chemical property data for alpha-, beta-, and gamma-hexachlorocyclohexane. In *Journal of Chemical and Engineering Data*, 2004; Vol. 49, pp 173-185.
2. Muir, D. C. G.; Teixeira, C.; Wania, F., Empirical and modeling evidence of regional atmospheric transport of current-use pesticides. *Environmental Toxicology and Chemistry* **2004,** *23* (10), 2421-2432;10.1897/03-457
3. Li, N.; Wania, F.; Lei, Y. D.; Daly, G. L., A Comprehensive and Critical Compilation, Evaluation, and Selection of Physical–Chemical Property Data for Selected Polychlorinated Biphenyls. *Journal of Physical and Chemical Reference Data* **2003,** *32* (4), 1545-1590;10.1063/1.1562632
4. Wania, F.; Dugani, C., Assessing the long-range transport potential of polybrominated diphenyl ethers: A comparison of four multimedia models. *Environmental Toxicology and Chemistry* **2003,** *22* (6), 1252-1261
5. Ni, N.; Yalkowsky, S. H., Prediction of Setschenow constants. *International Journal of Pharmaceutics* **2003,** *254* (2), 167-172;10.1016/S0378-5173(03)00008-5
6. Notz, D. Thermodynamic and Fluid-Dynamical Processes in Sea Ice (Ph.D Thesis). Ph.D, University of Cambridge, Cambridge, U.K., 2005.
7. Weast, R. C., *CRC handbook of chemistry and physics: a ready-reference book of chemical and physical data*. 52nd ed.; Chemical Rubber Co: Cleveland, Ohio, 1971.
8. Thomas, M. Brine and pressure dynamics in growing sea ice: first results from the Roland von Glasow air-sea-ice chamber. Ph.D, University of East Anglia, Norwich, U.K., 2019.
9. Rees Jones, D. W.; Worster, M. G., A physically based parameterization of gravity drainage for sea-ice modeling. *Journal of Geophysical Research: Oceans* **2014,** *119* (9), 5599-5621;10.1002/2013JC009296
10. Cox, G.; Weeks, W., Numerical simulations of the profile properties of undeformed first-year sea ice during the growth season. *Journal of Geophysical Research: Oceans* **1988,** *93* (C10), 12449-12460;10.1029/JC093iC10p12449
11. Griewank, P. J.; Notz, D., Insights into brine dynamics and sea ice desalination from a 1-D model study of gravity drainage. *Journal of Geophysical Research: Oceans* **2013,** *118* (7), 3370-3386;10.1002/jgrc.20247
12. Vancoppenolle, M.; Goosse, H.; De Montety, A.; Fichefet, T.; Tremblay, B.; Tison, J. L., Modeling brine and nutrient dynamics in Antarctic sea ice: The case of dissolved silica. *Journal of Geophysical Research: Oceans* **2010,** *115* (C2), n/a-n/a;10.1029/2009JC005369
13. Worster, M. G.; Rees Jones, D. W., Sea-ice thermodynamics and brine drainage. *Philosophical transactions. Series A, Mathematical, physical, and engineering sciences* **2015,** *373* (2045);10.1098/rsta.2014.0166
14. Notz, D.; Worster, M. G., In situ measurements of the evolution of young sea ice. *Journal of Geophysical Research: Oceans* **2008,** *113* (C3), n/a-n/a;10.1029/2007JC004333